Backstepping Control of a Magnetic Levitation System Using PSO

Yeabisra Wubishet ENGDA[1], Gang Gyoo JIN[2], Yung-Deug SON[3]*

[1] Department of Electrical Engineering, Dilla University, P.O. Box 419, Dilla, Ethiopia
wubyab@gmail.com

[2] Department of Electrical Power and Control Engineering, Adama Science and Technology University, P.O. Box 1888, Adama, Ethiopia
gjin30@gmail.com

[3] Department of Mechanical Facility Control Engineering, Korea University of Technology and Education, 1600 Chungjeol-ro, Dongnam-gu, Cheonan, Chungnam, 31253, Korea
ydson@koreatech.ac.kr (**Corresponding author*)

Abstract: Magnetic levitation systems are highly nonlinear and unstable systems and their efficacy depends on a well-designed controller for stabilizing the system and for tracking the desired reference signal. This work focuses on the design of a backstepping controller for a magnetic levitation (maglev) system under parameter uncertainty which is load variation. The mathematical model is obtained and the stable controller is designed based on this model and Lyapunov's theorem. Then, the controller parameters are optimally tuned by minimizing the integral of absolute error and control deviation performance criterion using the particle swarm optimization (PSO) algorithm. For comparison purposes, a Proportional-Integral (PI)-type linear quadratic regulator is also designed. A set of simulation works are carried out in order to verify both the tracking performance and the robustness against disturbance for the proposed controller.

Keywords: Magnetic levitation system, Backstepping control, PSO, PI-type linear quadratic regulator.

1. Introduction

Levitation is the process of suspending an object in the air in a stable position without any physical contact (Shu'aibu et al., 2017). It can be accomplished through the use of electric or magnetic forces. In a magnetic levitation system, an object (made of nickel, aluminum, iron, etc.) achieves equilibrium in air space under the influence of magnetic field only.

Magnetic levitation, also known as maglev, is an advanced technology in which an object is suspended or levitated in the midair with no support other than the magnetic field (Santhiya & Kishore, 2020). Due to the lack of contact with the levitated object, the magnetic levitation system (MLS) provides no wear and friction. Friction plays a significant role in real-world applications as it reduces performance in most cases. MLS is one of the approaches that has made a significant contribution to the reduction of friction (Banerjee et al., 2019). Many applications are focused on maglev technology since it is a non-contact technology that results in zero friction losses and higher energy efficiency. As a result, the cost of maintenance is low. MLS is used in frictionless bearings, high-speed ground transportation system, maglev heart pumps, maglev fans, space launching stations, wind turbines, high-precision positioning stages, and many other applications (Dalwadi et al., 2021). The most common application of this system is the magnetic levitation train.

The magnetic levitation (maglev) train is a new large-scale transportation system that uses magnetic fields to levitate, provide propulsion and direction. Due to technological advancements, it is becoming more viable in the public transport field, providing faster, more comfortable, and safer transportation than the conventional train (Braga Júnior & Barreiros, 2013). There are two different approaches for designing maglev train systems. The electrodynamic suspension (EDS) system is based on eddy current magnetic repulsive force, while the electromagnetic suspension (EMS) system is based on electromagnetic attractive force (Raj et al., 2019). EMS maglev train has unstable behaviour (Kim et al., 2017; Leng et al., 2019). Therefore, designing an excellent tracking controller is required to stabilize the train in the air and follow the desired reference signal in the presence of load variation.

Since suspension air gap control and following the desired reference signal are essential for the effective operation of the maglev system, several scholars and researchers have proposed a variety of control strategies and optimization techniques.

The system dynamic characteristics were analyzed in linear controllers, such as PID controller (Dey et al., 2020; Khan et al., 2018), FOPID controller (Mughees & Mohsin, 2020) and, state feedback controller (Awelewa et al., 2019), are based on

https://doi.org/10.24846/v32i3y202305

the linearized models, which are implemented in a small neighborhood near the equilibrium point. So, if the system deviates from equilibrium, the linearized model may become invalid. The high nonlinearity of the magnetic levitation train system makes the nonlinear controllers more desirable. In (Karabacak et al., 2023), the PID and LQR control were applied to a MLS, and their performances were compared. The PID parameters were calculated using the Matlab PID tuning function and the Q and R matrices of LQR control were chosen by the trial and error method. LQR control does not exceed the reference input and reaches the desired value in a considerably quicker period. Furthermore, disturbance effects achieve the reference input faster in LQR control. A comparative evaluation of magnetic levitation controllers employing the proportional-integral-derivative (PID) controller based optimal tuning was presented in (Abdalhadi et al., 2022). Three tuning strategies are investigated: radial basis function neural network (RBFNN) based metamodel, gradient descent, and standard PID based on Ziegler-Nichols tuning. The gradient descent algorithm gave the best rising time and overshoot in comparison with the RBFNN metamodel approach, hence the latter was the less successful method employed for tuning the PID controller in this paper.

In (Singh & Kumar, 2018), two control strategies, that is, PID controller and backstepping controller (BSC) were developed for the stabilization and control of a magnetic levitation system. The PID parameters were tuned with a model-based tuning algorithm, while BSC parameters were chosen by the trial and error method. The BSC approach achieved the desired control objective by providing better response and requiring less control effort than the PID controller while BSC parameters were chosen by the trial and error method. The robustness of the proposed control system was not tested in the paper. In (Adil et al., 2020), super-twisting and integral backstepping sliding mode controllers were proposed for controlling a maglev system and the system robustness was evaluated by adding external disturbance. The super-twisting SMC performed better than the integral backstepping SMC in terms of dynamic performance and robustness against disturbances. Jibril et al. (2020) investigated NARMA-L2, model reference and predictive controllers for a nonlinear magnetic levitation train. The simulation results showed that the magnetic levitation train system with the NARMA-L2 neuro controller has an effective performance with the lowest percentage overshoot compared with the other controllers.

This paper presents the mathematical model of a maglev train system. A BSC law is designed for obtaining desired tracking performance of the feedback system. The control law is designed to guarantee the global asymptotic stability of the nonlinear system regardless of load disturbance changes present in the system. The parameters of the controller are tuned using particle swarm optimization (PSO) so that the integral of absolute error and control deviation (IAEU) performance criterion is minimized. By penalizing both large errors and large control inputs, the proposed controller is tuned to optimize the trade-off between the tracking error and control effort. Meanwhile, the proportional-Integral (PI)-type LQR is designed for comparison purpose and the Q and R matrices are determined by the trial and error method. A set of simulation works are carried out to validate the effectiveness of the proposed control method by comparing it with that of the PI-type LQR controller.

The paper is organized as follows. Section 2 presents the mathematical model of the maglev train system. Section 3 provides the details about the design of the BSC for the maglev train system. Section 4 discusses the simulation results and Section 5 contains the conclusion of this work.

2. The Modelling of a Magnetic Levitation System

This section focuses on the analysis of a single-point suspension of the EMS train system using a single electromagnet system, which is helpful in understanding the behavior of the entire levitation system. Figure 1 depicts the simplified model of the single electromagnet suspension.

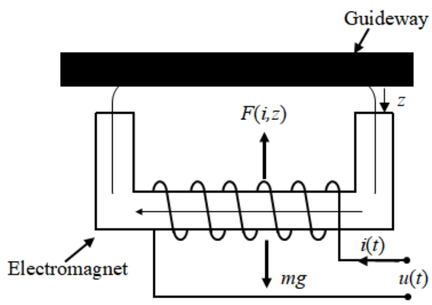

Figure 1. Simplified model of the single electromagnet suspension

The suspension of an MLS roughly comprises the mechanical and electrical subsystems. The mechanical subsystem represents the system's vertical motion. Newton's second law of motion is applied for obtaining the model, where the upward direction is assumed to be negative. Considering all balancing forces acting on the levitated system, the following equation of motion is obtained:

$$m\frac{d^2z}{dt^2} = -f_{mag} + mg \tag{1}$$

where z is the levitation gap between the track and the electromagnet, m is the mass of the maglev train, g is the acceleration due to gravity and f_{mag} is the electromagnetic force, denoted as $F(i,z)$ in Figure 1.

The electromagnetic force can be expressed by

$$f_{mag} = \frac{\mu_0 N^2 i^2 A}{4z^2} \tag{2}$$

where μ_0 is the permeability of free space, N is the number of turns of the coil, i is the coil current of the suspension electromagnet and A is the cross-section area of the magnetic path.

Substituting equation (2) into equation (1) gives

$$m\frac{d^2z}{dt^2} = -\frac{\mu_0 N^2 i^2 A}{4z^2} + mg \tag{3}$$

In addition, the voltage equation in the electromagnet winding circuit can be derived using the Kirchhoff's voltage law as in (Alkurawy, 2019).

$$Ri(t) + \frac{\mu_0 N^2 A}{2z(t)}\frac{di(t)}{dt} - \frac{\mu_0 N^2 A i(t)}{2z^2(t)}\frac{dz(t)}{dt} = u(t) \tag{4}$$

where u is the applied voltage input and R is the magnetic reluctance of the circuit.

Defining the state variables as $x_1(t)= z(t)$, $x_2(t)= (t)$, and $x_3(t)= i(t)$ gives the model in state space form as

$$\dot{x}_1(t) = x_2(t) \tag{5a}$$

$$\dot{x}_2(t) = -a\frac{x_3^2(t)}{x_1^2(t)} + g \tag{5b}$$

$$\dot{x}_3(t) = \frac{x_3(t)x_2(t)}{x_1(t)} - \frac{Rx_3(t)x_1(t)}{k} + \frac{x_1(t)}{k}u(t) \tag{5c}$$

$$y(t) = x_1(t) \tag{5d}$$

where $k = \frac{\mu_0 N^2 A}{2}$ and $a = \frac{k}{2m}$.

From equations (5a-d), the state variables and the control input at an operating point, $y = yr$, become

$$x_{10} = y_r, x_{20} = 0, x_{30} = x_{10}\sqrt{\frac{g}{a}}, u_0 = Rx_{30} \tag{6}$$

It is assumed that the motion of the equations (5a-d) is in the neighborhood of the operating point, that is

$$\Delta x = x - x \tag{7a}$$

$$\Delta u = u - u_0 \tag{7b}$$

$$\Delta y = y - y_r \tag{7c}$$

where Δx, Δu, and Δy are small deviations of x, u, and y, respectively. The nonlinear system can be linearized around (x_0, u_0).

$$\Delta\dot{x} = A\Delta x + B\Delta u \tag{8a}$$

$$\Delta y = C\Delta x \tag{8b}$$

where

$$A = \begin{bmatrix} 0 & 1 & 0 \\ \frac{2ax_{30}}{x_{10}^3} & 0 & \frac{-2ax_{30}}{x_{10}^2} \\ -\frac{Rx_{30}}{k} + \frac{u_0}{k} & \frac{x_{30}}{x_{10}} & -\frac{Rx_{10}}{k} \end{bmatrix}, B = \begin{bmatrix} 0 \\ 0 \\ \frac{x_{10}}{k} \end{bmatrix},$$

$$C = \begin{bmatrix} 1 & 0 & 0 \end{bmatrix} \tag{8c}$$

3. Controller Design

3.1 Backstepping Controller Design

Backstepping is a recursive method that uses a systematic design approach and the Lyapunov controller design functions for particular types of nonlinear dynamical systems (Bai et al., 2013; Basri et al., 2018; Singh & Kumar, 2018).

Firstly, the following error is considered:

$$e_1 = y_r - x_1 \tag{9}$$

The time derivative of the error is:

$$\dot{e}_1 = \dot{y}_r - \dot{x}_1 = \dot{y}_r - x_2 \tag{10}$$

Considering x_2 as virtual control law w_1, equation (10) can be rewritten as:

$$\dot{e}_1 = \dot{y}_r - w_1 \tag{11}$$

For the stability analysis of equation (11), the candidate Lyapunov function is considered:

$$V_1 = \frac{1}{2}e_1^2 \tag{12}$$

Differentiating equation (12) and substituting Equation (11) into equation (12) yields:

$$\dot{V}_1 = e_1(\dot{y}_r - w_1) \tag{13}$$

If the virtual control law $w1$ is expressed as:

$$w_1 = \dot{y}_r + k_1 e_1 \tag{14}$$

where $k1$ is a positive design parameter, then equation (13) becomes $\dot{V}_1 = -k_1 e_1^2 < 0$.

This means that according to Lyapunov stability theorem, the closed-loop system of equation (11) with equation (14) is globally asymptotically stable.

For backstepping control, the change of variable is used as:

$$e_2 = x_2 - w_1 = x_2 - \dot{y}_r - k_1 e_1 \tag{15}$$

Namely,

$$x_2 = e_2 + \dot{y}_r + k_1 e_1 \tag{16}$$

From equation (10) and equation (16), the following is obtained:

$$\dot{e}_1 = \dot{y}_r - x_2 = -e_2 - k_1 e_1 \tag{17}$$

Differentiating equation (15) and substituting equations (5b) and (17) into equation (15) yields:

$$\begin{aligned} \dot{e}_2 &= -a\frac{x_3^2}{x_1^2} + g - \ddot{y}_r - k_1\dot{e}_1 \\ &= -a\frac{x_3^2}{(y_r - e_1)^2} + g - \ddot{y}_r + k_1(e_2 + k_1 e_1) \end{aligned} \tag{18}$$

Considering $x3$ as virtual control law $w2$, equation (18) can be rewritten as:

$$\dot{e}_2 = -a\frac{w_2^2}{(y_r - e_1)^2} + g - \ddot{y}_r + k_1(e_2 + k_1 e_1) \tag{19}$$

The second Lyapunov function shall be considered as:

$$V_2 = \frac{1}{2}(e_1^2 + e_2^2) \tag{20}$$

Accordingly, the time derivative of $V2$ can be obtained as:

$$\begin{aligned} \dot{V}_2 &= e_1\dot{e}_1 + e_2\dot{e}_2 \\ &= -k_1 e_1^2 + e_2\left(-e_1(1-k_1^2) - a\frac{w_2^2}{(y_r - e_1)^2}\right) \\ &\quad + e_2\left(k_1 e_2 + g - \ddot{y}_r\right) \end{aligned} \tag{21}$$

If the virtual control law w_2 is expressed in such a way that $\dot{V}_2$ is negative definite,

$$w_2 = (y_r - e_1)\sqrt{q} \tag{22a}$$

$$q = \frac{1}{a}\left(g - \ddot{y}_r + e_2(k_1 + k_2) - e_1(1 - k_1^2)\right) \tag{22b}$$

where *k2 is a positive* design parameter. Then substituting equations (22a-b) into equation (21) gives $\dot{V}_2 = -k_1 e_1^2 - k_2 e_2^2 < 0$.

It is clear that $\dot{V}_2$ is negative definite. Thus, the closed-loop system of equation (19) with equation (22) is globally asymptotically stable.

Finally, the change of variable is used as:

$$e_3 = x_3 - w_2 = x_3 - (y_r - e_1)\sqrt{q} \tag{23}$$

Namely,

$$x_3 = e_3 + (y_r - e_1)\sqrt{q} \tag{24}$$

By taking the time derivative of equation (23) and substituting equation (5c), the following is obtained:

$$\begin{aligned} \dot{e}_3 &= \dot{x}_3 - \dot{w}_2 \\ &= \frac{x_3 x_2}{x_1} - \frac{R x_3 x_1}{k} + \frac{1}{k}x_1 u - \dot{w}_2 \end{aligned} \tag{25}$$

Substituting equations (9), (16) and (24) into equation (25) yields:

$$\begin{aligned} \dot{e}_3 = &\frac{\left(e_3 + (y_r - e_1)\sqrt{q}\right)\left(e_2 + \dot{y}_r + k_1 e_1\right)}{(y_r - e_1)} \\ &- \frac{\mathrm{R}\left(e_3 + (y_r - e_1)\sqrt{q}\right)(y_r - e_1)}{k} \\ &+ \frac{1}{k}(y_r - e_1)u - \dot{w}_2 \end{aligned} \tag{26}$$

The Lyapunov function for the overall system is considered as:

$$V_3 = \frac{1}{2}(e_1^2 + e_2^2 + e_3^2) \tag{27}$$

Computing the time derivative of $V3$ and substituting equations (17), (18), (24) and (26) into equation (27) yields:

$$\begin{aligned} \dot{V} = &\; e_1\dot{e}_1 + e_2\dot{e}_2 + e_3\dot{e}_3 \\ = &-k_1 e_1^2 - k_2 e_2^2 + e_3\left(\frac{1}{k}(y_r - e_1)u - \dot{w}_2\right) \\ &+ e_3\left(-\frac{a e_2}{(y_r - e_1)^2}\left(e_3 + 2(y_r - e_1)\sqrt{q}\right)\right) \\ &+ e_3\left(\frac{\left(e_3 + (y_r - e_1)\sqrt{q}\right)\left(e_2 + \dot{y}_r + k_1 e_1\right)}{(y_r - e_1)}\right) \end{aligned} \tag{28}$$

If the applied voltage input u is selected in such a way that $\dot{V}_3$ is negative definite,

$$u=\frac{k}{(y_r-e_1)}\left(\frac{ae_2}{(y_r-e_1)^2}\left(e_3+2(y_r-e_1)\sqrt{q}\right)\right.$$
$$-\frac{k\left(e_2+\dot{y}_r+k_1e_1\right)}{(y_r-e_1)}\left(\frac{\left(e_3+(y_r-e_1)\sqrt{q}\right)}{(y_r-e_1)}\right) \quad (29)$$
$$\left.+\frac{k}{(y_r-e_1)}\left(\dot{w}_2-k_3e_3\right)+R\left(e_3+(y_r-e_1)\sqrt{q}\right)\right.$$

where $\dot{w}_2$ is computed by

$$\dot{w}_2=\left(\dot{y}_r-\dot{e}_1\right)\sqrt{q}+(y_r-e_1)\frac{\dot{q}}{2\sqrt{q}} \quad (30)$$

$$\dot{q}=\frac{1}{a}\left(-\ddot{y}_r+\dot{e}_2(k_1+k_2)-\dot{e}_1\left(1-k_1^2\right)\right) \quad (31)$$

then

$$\dot{V}_3=-k_1e_1^2-k_2e_2^2-k_3e_3^2 \quad (32)$$

It is clear that $\dot{V}_3$ is negative definite and the overall closed-loop system is globally asymptotically stable.

3.2 Controller Parameter Tuning

As it is known from the previous subsection, the designed backstepping controller has three parameters, k_1, k_2 and k_3 that affect the performance of the maglev train system. The tuning of these parameters leads to a multivariate optimization problem and needs the selection of an appropriate objective function. In this work, the IAEU performance criterion is adopted as the objective function. IAEU can avoid an excessive control input when the setpoint and/or disturbances change abruptly (Durand et al., 2014).

It is defined as:

$$\mathrm{IAEU}=\int_0^{t_f}\left(|e(t)|+w|\Delta u|\right)dt \quad (33)$$

where e is the error, that is, the difference between the reference input and the output with $e = y_r - y$ and Δu is the deviation of the control input from u_0 with $\Delta_u = u - u_0$ where u_0 is obtained from equation (6) and w is the weighting factor. Once the objective function is chosen, the next step is to apply the optimization method. In this study, the PSO algorithm is used for tuning the three design parameters. Figure 2 shows block diagram for offline-tuning the BSC using the PSO algorithm.

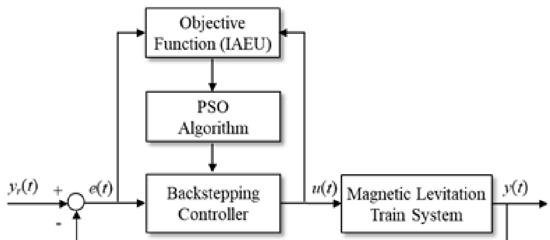

Figure 2. Offline-tuning of the backstepping controller using PSO

3.3 PI-Type Linear Quadratic Regulator

For comparison purposes, a linear quadratic regulator (LQR) is designed based on the linearized model in equations (8a-c). In order to eliminate the steady-state error and design a tracking controller, a new state variable is added as:

$$z=\int(y-y_r)dt \quad (34)$$

where y_r is the setpoint. Differentiating Equation (34) and combining it with equation (8a) gives the following augmented model:

$$\Delta\dot{\tilde{x}}=\tilde{A}\Delta\tilde{x}+\tilde{B}\Delta u+\begin{bmatrix}0\\-1\end{bmatrix}(y_r+x_{10}) \quad (35a)$$

where

$$\Delta\tilde{x}=\begin{bmatrix}\Delta x\\ z\end{bmatrix},\ \tilde{A}=\begin{bmatrix}A & 0\\ C & 0\end{bmatrix}\text{ and }\tilde{B}=\begin{bmatrix}B\\0\end{bmatrix} \quad (35b)$$

Then, the feedback control law is represented as follows:

$$\Delta u=-\tilde{K}\Delta\tilde{x} \quad (36)$$

The gain matrix $\tilde{K}$ can be obtained in several ways, but here the optimal control technique is applied so that the quadratic cost function is minimized:

$$J=\int_0^{\infty}(\Delta\tilde{x}^T\tilde{Q}\Delta\tilde{x}+\Delta u^T\tilde{R}\Delta u)dt \quad (37)$$

where $\tilde{Q}$ is a positive semi-definite matrix and $\tilde{R}$ is a positive definite matrix. Then $\tilde{K}$ can be obtained from:

$$\bar{K}=-\tilde{R}^{-1}\tilde{B}^T\tilde{P}\,. \quad (38)$$

where $\tilde{P}$ is the solution of the algebraic Riccati equation:

$$\tilde{P}\tilde{A}+\tilde{A}^T\tilde{P}-\tilde{P}\tilde{B}\tilde{R}^{-1}\tilde{B}^T\tilde{P}+\tilde{Q}=0 \quad (39)$$

Rewriting equation (36) results in:

$$u=u_0-K_1(x-x_0)+k_i\int(y_r-y)dt \quad (40)$$

where $\tilde{K}=\left[K_1 \quad k_i\right]$.

4. Simulation and Discussion

The parameter values for simulation are the same as used in (Xu et al., 2017) and (Xu et al., 2018).

The initial position of the suspension air gap used in this work is 10mm, which was selected based on the operating range. With this selection, u_0 = 25.45.

Table 1. Physical parameter values of the magnetic levitation train system

Parameters with symbol	Values with unit
Mass of the EMS train (m)	700kg
Cross-section area of the magnetic path (A)	0.024m^2
Number of turns of the coil (N)	450
Magnetic reluctance of the magnetic circuit (R)	1.2Ω
Permeability of free space (μ_0)	$4\pi\times10^{-7}$H/m

4.1 Parameter Settings of the Controllers

In order to tune the proposed controller optimally, the particle swarm optimization function in MATLAB is used for adjusting the controller parameters k_1, k_2 and k_3. The parameters were chosen within the bound $0 \le k_1, k_2, k_3 \le 80$ with $w = 0.2\times10\text{-}3$. The average values for running the program 20 times with different random seeds are k_1 = 33.542, k_2 = 33.673 and k_3 = 31.160. Figure 3 shows a typical example of the optimization process for the BSC with PSO.

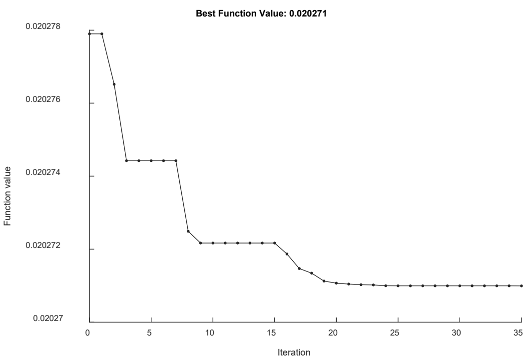

Figure 3. Optimization process of the BSC with PSO

For LQR, the weighting matrices were selected by the trial and error method as:

$$\tilde{Q} = diag(50,1,1,9\times10^{8}) \text{ and } \tilde{R} = 1\times10^{-3}$$

that results in:

$$\tilde{K} = 1\times10^{5}[-2.3595, -0.0426, 0.0006, -9.4868].$$

4.2 Tracking Performance Test

The tracking performance of the backstepping controller was assessed for different step inputs without load variation. For this test, the suspension air gap was increased from 10mm to 12mm. The responses of the proposed controller were compared with those of the LQR controller. Figure 4 shows the responses obtained by the two controllers for the upward change of the setpoint. In order to gauge the setpoint tracking performance of the two control methods quantitatively, overshoot M_p, rise time t_r, 2% settling time t_s, and IAEU were obtained. Table 2 illustrates the values obtained for the above-mentioned performance indices for the upward change of the setpoint. Figure 5 shows the responses of the two methods when the setpoint was decreased from 10mm to 8mm. Table 3 shows the quantitative performances of the two controllers for the downward change of the setpoint.

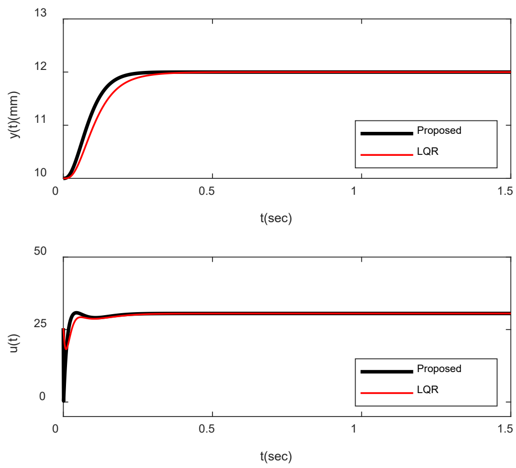

Figure 4. Responses of the proposed and LQR controllers for the upward change of the setpoint

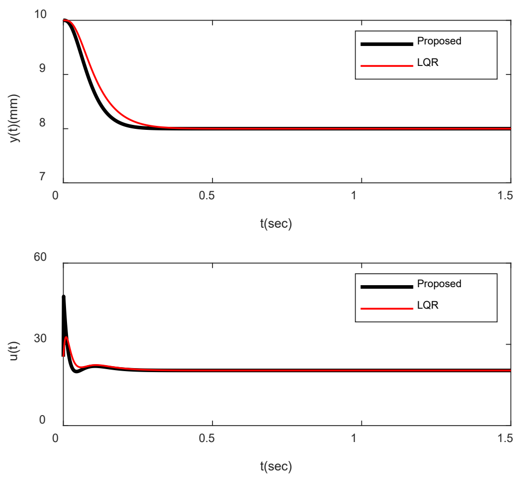

Figure 5. Responses of the proposed and LQR controllers for the downward change of the setpoint

Table 2. Tracking performance for the upward change of the setpoint

Controller	Performance indices			
	M_p	t_r	t_s	IAEU
Proposed	0	0.128	0.190	0.181
LQR	0	0.173	0.267	0.245

Table 3. Tracking performance for the downward change of the setpoint

Controller	Performance indices			
	M_p	t_r	t_s	IAEU
Proposed	0	0.129	0.193	0.183
LQR	0	0.176	0.267	0.245

As it can be seen from Figures 4 and 5 and from Tables 2 and 3, both controllers have no overshoot but the transient response of the BSC shows a better tracking performance with t_r = 0.128s, t_s= 0.190s and IAEU = 0.181 for upward, and t_r = 0.129s, t_s = 0.193s and IAEU = 0.183 for downward setpoint changes, respectively.

So, it is clear from these numerical indicators that the BSC has a better tracking performance for the given setpoint changes when compared with the LQR controller.

4.3 Performance Test Against Load Variation

The suspension must support the total mass of the train which includes both the vehicle's mass and the load (weight of passengers). In this work, the load variations of 10 and 30% of the total mass are considered. Figure 6 shows the robustness of the two control methods in the presence of mass changes of 10% and 30%. As it can be seen in Figure 6, both control methods satisfactorily follow the reference signal with an internal disturbance of 70kg and a load mass of 210kg. However, the results clearly show that the proposed backstepping controller settles faster than the LQR controller.

In order to assess the disturbance rejection performance of the two methods quantitatively, the perturbance peak M_{peak}, peak time t_{peak}, recovery time t_{rcy} and IAEU in equation (33) are used. M_{peak} means $|y_{max} - y_r|$ and t_{rcy} denotes the time that it takes for y to recover within 2% of y_r. A comparison of the performances of both control strategies for a 10% and a 30% increase in load mass is illustrated in Tables 4 and 5, respectively. It can be seen from these tables that the BSC has a better response with smaller values of M_{peak}, t_{peak}, t_{rcy}, and IAEU for increase in load mass. These numerical performances indicate that the BSC shows a higher robustness under load variations than the LQR controller.

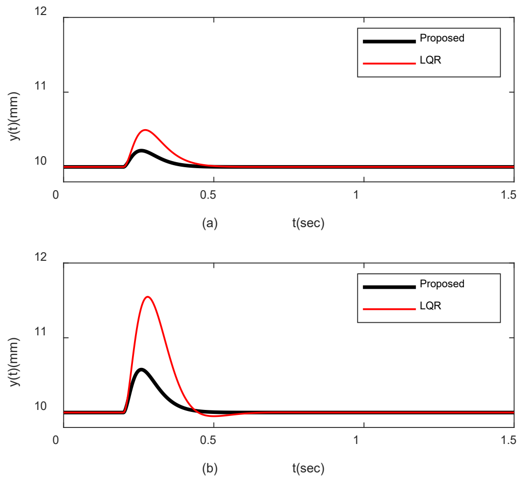

Figure 6. Responses of the proposed and the LQR controller for: a) a 10% increment of *m*; b) a 30% increment of *m*

Table 4. Performance measures against load variation for a 10% increment of *m*

Controller	Performance indices			
	M_{peak}	t_{peak}	t_{rcy}	IAEU
Proposed	0.218	0.018	0.269	0.024
LQR	0.494	0.294	0.307	0.063

Table 5. Performance measures against load variation for a 30% increment of *m*

Controller	Performance indices			
	M_{peak}	t_{peak}	t_{rcy}	IAEU
Proposed	0.574	0.059	0.269	0.064
LQR	1.548	0.080	0.357	0.194

5. Conclusion

In this paper, a nonlinear backstepping control scheme based on Lyapunov's theorem was studied for a maglev levitation system and the controller parameters were optimally tuned by minimizing the IAEU performance criterion using PSO. The main results derived from a set of simulation studies on the nonlinear model are as follows.

First, the BSC not only has no overshoot but also outperforms the LQR by reducing t_s by 28.8% and 27.7%, and IAEU by 26.1% and 25.3%, for upward and downward setpoint changes, respectively.

Second, for robustness against load change of 10%, the BSC achieves a better performance than the LQR controller by reducing the overshoot by 55.9%, peak time by 93.9%, the recovery time by 12.4%, and IAEU by 61.9% in comparison with the results obtained for the LQR. As for robustness against a load change of 30%, the BSC also achieves a better performance than the LQR by reducing M_{peak} by 55.9%, t_{peak} by 26.3%, t_{rcy} by 24.6%, and IAEU by 67.0%.

In conclusion, the BSC shows a better setpoint tracking and load disturbance rejection performance than the LQR controller.

Future research can focus on simplifying the control algorithm using a nonlinear transformation and implementing it in a real system.

Acknowledgements

This paper was supported by the Education and Research promotion program of KOREATECH in 2023.

REFERENCES

Abdalhadi, A., Wahid, H. & Burhanuddin, D. H. (2022) An optimal proportional integral derivative tuning for a magnetic levitation system using metamodeling approach. *Indonesian Journal of Electrical Engineering and Computer Science*. 25(3), 1356-1366. doi: 10.11591/ijeecs.v25.i3.

Adil, H. M. M., Ahmed, S. & Ahmad, I. (2020) Control of MagLev System Using Supertwisting and Integral Backstepping Sliding Mode Algorithm. *IEEE Access*. 8, 51352–51362. doi: 10.1109/ACCESS.2020.2980687.

Alkurawy, L. E. J. (2019) Simulation of Robust Control of Magnetic Levitation System. *Journal of Engineering and Applied Sciences*. 14(13), 4523-4531. doi: 10.36478/jeasci.2019.4523.4531.

Awelewa, A. A., Popoola, O. & Ademola, A. (2019) Nonlinear dynamic simulation of a magnetic levitation system using MATLAB/Simulink. *International Journal of Engineering Research and Technology*. 12(12), 2143-2158.

Bai, R., Tong, S. & Karimi, H. R. (2013) Modeling and backstepping control of the electronic throttle system. *Mathematical Problems in Engineering*. 2013, 871674. doi: 10.1155/2013/871674.

Banerjee, S., Mukherjee, R., Mukheriee, M., Sengupta, S. & Pandey, S. (2019) Operating Frequency Enhancement of Magnetic levitation system using fractional order $PI^{\lambda}D^{\mu}$ Controller: Design and Tuning. In: *Proceedings of 2019 IEEE International Conference on Distributed Computing, VLSI, Electrical Circuits and Robotics, DISCOVER 2019, 11-12 August, 2019, Manipal, India*. IEEE Bangalore Section. pp. 1-6.

Basri, M. A. M., Abidin, M. S. Z. & Subha, N. A. M. (2018) Simulation of Backstepping-based Nonlinear Control for Quadrotor Helicopter. *Applications of Modelling and Simulation*. 2, 34-40.

Dalwadi, N., Deb, D. & Muyeen, S. M. (2021) A reference model assisted adaptive control structure for maglev transportation system. *Electronics*. 10(3), 332. doi: 10.3390/electronics10030332.

Dey, S., Dey, J. & Banerjee, S. (2020) Optimization Algorithm Based PID Controller Design for a Magnetic Levitation System. In: *Proceedings of the 2020 IEEE Calcutta Conference, CALCON 2020, 28-29 February, 2020, Kolkata, India*. pp. 258-262.

Durand, S., Boisseau, B., Martinez-Molina, J. J., Marchand, N. & Raharijaona, T. (2014) Event-based LQR with integral action. In: *Proceedings of 19th IEEE International Conference on Emerging Technologies and Factory Automation, ETFA 2014, 16-19 September, 2014, Barcelona, Spain*. IEEE.

Braga Júnior, G. F. & Barreiros, J. A. L. (2013) PID Control Design for a Maglev Train System. *Applied Mechanics and Materials*. 389, 425-429. doi: 10.4028/www.scientific.net/AMM.389.425.

Jibril, M., Tadese, E. A., Tadese, M., Dawa, D. & Dawa, D. (2020) Comparison of Neural Network Based Controllers for Nonlinear EMS Magnetic Levitation Train. *Control Theory and Informatics.* 10, 13-18. doi: 10.7176/cti/10-02.

Karabacak, Y., Yaşar, A. & Saritaş, İ. (2023) Performance Comparison of PID and LQR Controllers for Control of Non-Linear Magnetic Levitation System. *Dokuz Eylul University Faculty of Engineering Journal of Science and Engineering.* 25(74), 339-350.doi: 10.21205/deufmd.2023257407.

Khan, M. K. A. A., Manzoor, S., Marais, H., Aramugam, K., Elamvazuthi, I. & Parasuraman, S. (2018) PID Controller design for a Magnetic Levitation system. In: *Proceedings of 2018 IEEE 4th International Symposium in Robotics and Manufacturing Automation, ROMA 2018, 11-12 December, 2018, Perambalur, India*. pp. 1-5.

Kim, M., Jeong, J. H., Lim, J., Kim, C. H. & Won, M. (2017) Design and control of levitation and guidance systems for a semi-high-speed maglev train. *Journal of Electrical Engineering and Technology*. 12(1), 117-125. doi: 10.5370/JEET.2017.12.1.117.

Leng, P., Yu, P., Gao, M., Li, J. & Li, Y. (2019) Optimal control scheme of maglev train based on the disturbance observer. In: *Proceedings of 38th Chinese Control Conference, CCC*, *2019, 27-30 July, 2019*, Guangzhou, China. pp. 1935-1940.

Mughees, A. & Mohsin, S. A. (2020) Design and Control of Magnetic Levitation System by Optimizing Fractional Order PID Controller Using Ant Colony Optimization Algorithm. *IEEE Access*. 8, 116704-116723. doi: 10.1109/ACCESS. 2020.3004025.

Raj, R., Swain, S. K. & Mishra, S. K. (2019) Optimal Control for Magnetic Levitation System Using H-J-B Equation Based LQR. In: *Proceedings of 2nd International Conference on Energy, Power and Environment: Towards Smart Technology, ICEPE 2018*, *1-2 June, 2018, Shillong, India*. pp. 1-6.

Santhiya, M. & Kishore, S. (2020). Design of Neuro PID Controller and State Feedback Controller for Magnetic Levitation System. In: *Proceedings of the 2020 IEEE International Conference on Communication and Signal Processing, ICCSP 2020*, *28-30 July, 2020, Chennai, India*. Piscataway, New Jersey, pp. 996-1001.

Shu'aibu, D., Rabiu, H. & Shehu, N. (2017) Efficient fuzzy logic controller for magnetic levitation systems. *Nigerian Journal of Technological Development*. 13(2), 50. doi: 10.4314/njtd.v13i2.2.

Singh, B. K. & Kumar, A. (2018) Backstepping Approach based Controller Design for Magnetic Levitation System. In: *Proceedings of 2018 5th IEEE Uttar Pradesh Section International Conference on Electrical, Electronics and Computer Engineering, UPCON 2018*, *2-4 November, 2018, Gorakhpur, India*. pp. 1–6.

Xu, J., Chen, C., Gao, D., Luo, S. & Qian, Q. (2017) Nonlinear dynamic analysis on maglev train system with flexible guideway and double time-delay feedback control. *Journal of Vibroengineering*. 19(8), 6346-6362. doi: 10.21595/jve.2017.18970.

Xu, J., Sun, Y., Gao, D., Ma, W., Luo, S. & Qian, Q. (2018) Dynamic Modeling and Adaptive Sliding Mode Control for a Maglev Train System Based on a Magnetic Flux Observer. *IEEE Access*. 6(c), 31571–31579. doi: 10.1109/ACCESS. 2018. 2836348.